

DEBRIS-FAN CONSTRICTIONS AND FLOOD HYDRAULICS IN RIVER CANYONS: SOME IMPLICATIONS FROM TWO-DIMENSIONAL FLOW MODELLING

ANDREW J. MILLER

Department of Geography, University of Maryland Baltimore County, Baltimore, Maryland 21228-5398, U.S.A.

Received 17 March 1993

Revised 5 September 1993

ABSTRACT

Rapids in river canyons are frequently found at sites where debris fans constrict flow along the channel. Whereas some fans may have persisted in the same location with unchanging geometry for centuries to millennia, others have changed in response to flow conditions imposed by successive floods. Such a change in boundary conditions may alter local flow hydraulics. This paper utilizes two-dimensional flow modelling to compare flood hydraulics along two alternative versions of an idealized reach of a river canyon: one with uniform width, gradient and cross-section, and a second perturbed by a prominent debris fan along the valley wall. The flow pattern along the reach with the fan is far more complex than the pattern along the uniform reach. Maximum velocity along the debris-fan reach is up to 50 per cent higher than along the uniform reach, maximum bed shear stress is up to three or four times higher, and an area of supercritical flow is predicted extending from the nose of the fan into the zone of flow expansion immediately downstream.

Comparison of model output along longitudinal profiles of the two reaches indicates that the backwater effect of the fan extends several valley widths upstream. Predicted flows based on the same stage are as much as 190 to 230 per cent greater along the uniform reach than along the debris-fan reach. Reconstruction of palaeoflood discharge based on remnant flood marks in the vicinity of the fan would be sensitive to assumptions about boundary conditions that existed in the past; this effect relaxes over a longitudinal distance of several hundred metres. Furthermore there are significant cross-stream gradients that change slope and direction several times in the vicinity of the fan, calling into question the utility of one-dimensional step-backwater hydraulic models for predicting high-water marks in areas of complex valley morphology.

KEY WORDS Flood Hydraulics Flow modelling Debris fan

INTRODUCTION

It is well known that most of the vertical drop and most of the energy loss along the longitudinal profiles of canyon rivers occurs at rapids (Leopold, 1969, p. 138). Rapids may be associated with planform constrictions and expansions of the channel as well as with vertical discontinuities in the bed profile. Constrictions often form at sites where debris fans, created by delivery of coarse sediment from steep tributary valleys, impinge on the main channel. A prominent example is provided by the Colorado River: according to Graf (1979), 79 per cent of the rapids along the Grand Canyon and 68 per cent of the rapids in 10 canyons of the Colorado River system are located at the mouths of tributaries. Kieffer (1985) notes that the Colorado River passes about 60 large debris fans formed in tributary floods in the first 400 km below Lee's Ferry, Arizona.

The flow pattern around such fans is characterized by flow separation and recirculation zones, which in turn are associated with characteristic types of sediment deposits (Schmidt, 1990). At the upstream end of a rapid, there is commonly a critical-flow section, with a short stretch of supercritical flow terminated by a transition back to subcritical flow in a hydraulic jump at the downstream end. Patterns of scour and deposition in the vicinity of the rapid are influenced by the locations of accelerating and decelerating flow.

The pattern of flow around a debris fan during a large flood exerts influence on the shape of the water surface in the immediate vicinity of the fan and for some distance upstream and downstream. If the fan is a relatively permanent feature, hydraulic conditions for any specified flow may be considered predictable. Whether or not a fan is present, it should be possible to construct stage-discharge relations at locations along the channel using present morphology to define boundary conditions for use with hydraulic models. In combination with palaeostage indicators, such as slackwater deposits, erosion scars and silt lines, one-dimensional flow models based on the energy equation are useful in reconstructing the sequence of past floods in river canyons (Kochel and Baker, 1982; Baker *et al.*, 1983; O'Connor *et al.*, 1986; Partridge and Baker, 1987). As the ensuing analysis shows, however, there may be substantial longitudinal and cross-stream perturbations in the water surface that limit the effectiveness of one-dimensional models for predicting stage at the immediate vicinity of fans or other comparable irregularities in the channel. The complex flow pattern around a fan and the general sensitivity of flood-flow patterns to changes in topographic features merit further attention.

The particular boundary conditions affecting local hydraulics at a tributary confluence at any time depend, in part, on the temporal sequence of tributary floods and debris flows that create or augment debris

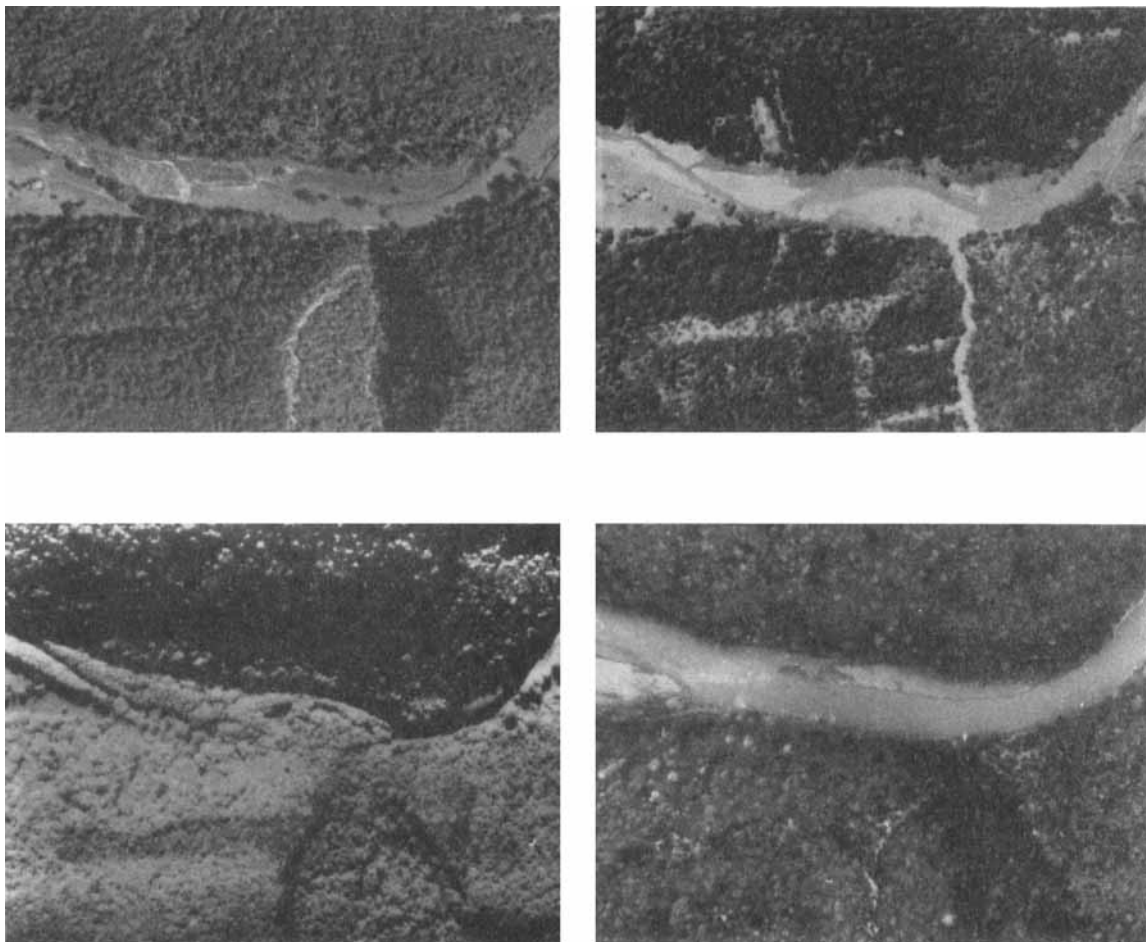


Figure 1. Sequence of four aerial photographs showing changes at a canyon locations along the South Branch Potomac River at a site upstream of Petersburg, West Virginia, where a debris fan formed in 1949 and was completely removed in 1985. Cross-sections surveyed in 1988 upstream and downstream from the tributary mouth revealed the presence of a deep scour hole where the fan had been prior to the 1985 flood. (a) 1945; (b) 1952 (debris fan in centre was formed in 1949); (c) September 1985; (d) November 1985 (debris fan removed in 1985 flood)

fans and main-stem floods that scour or destroy fans. Kieffer (1985) demonstrates that hydraulic conditions created by the interaction between a debris-fan constriction and flood flow can generate velocities exceeding the threshold required for transport of major boulders. When this happens the river is capable of modifying the shape of the fan. Widening of the channel may reach a point where even the largest subsequent flows cannot attain threshold erosion velocities.

In the central Appalachians, as along the Colorado River, the formation and the relative longevity of debris fans are dependent on both the frequency and the sequence of rare floods and debris flows. Fans in the Blue Ridge of Virginia, described by Kochel (1987), may have persisted for 11 000 years, modified primarily by infrequent debris flows with recurrence intervals of 3000–4000 years. In contrast, small fans and debris deposits in one area of the Valley and Ridge of West Virginia have been created and destroyed within a timespan of only four decades (Figures 1 and 2). Of a series of debris deposits that impinged on the main channel of the South Branch Potomac River and the North Fork South Branch Potomac River as a result of an intense convectional storm in 1949, most were removed or substantially modified by a subsequent flood in 1985, which generated few large debris avalanches but attained much larger discharges in the main valleys (Miller, 1990). Most of the surviving fans were located on or in the lee of floodplain segments where they were protected from the higher velocities attained in the channel.

This paper is predicated on the assumption that debris fans at tributary confluences are common along canyon rivers, that they have the potential to influence local flood hydraulics, and that fan morphology may change over time, thus altering the boundary conditions that affect flow patterns. The question I pose here is, how might hydraulic conditions differ in the presence or absence of a prominent debris fan? In order to explore this question I have chosen an idealized canyon reach with specified width, gradient and cross-sectional form. The dimensions and cross-sectional form of this reach are roughly comparable to sites observed in the South Branch Potomac River drainage. My approach is to simulate flood flow patterns, using a two-dimensional finite-element flow model, and to compare the hydraulics of flow in two realizations of the valley reach: one that includes a large debris fan protruding from the valley wall and one that does not. In particular, I examine the effects of the fan on longitudinal and cross-stream water-surface profiles and on stage-discharge relations at several locations along the modelled reach. Implications for the patterns of scour and deposition in the vicinity of the fan and for palaeohydrologic reconstruction of past floods are addressed below.

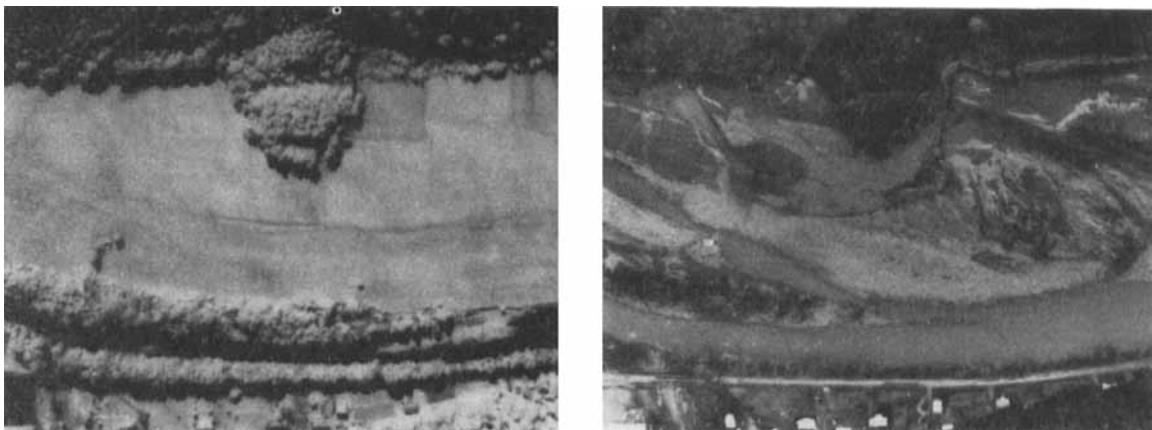


Figure 2. (a) Vegetated debris fan on floodplain of North Fork South Branch Potomac River at mouth of unnamed tributary. Debris fan formed in June 1949; photograph taken in September 1985. (b) Same site after November 1985 flood; although this fan was not removed by the 1985 flood, a large scour mark was incised in the floodplain as overbank flow was diverted around it. Photograph taken in November 1985

FLOW MODEL

The flow model used in this study is RMA2 (King, 1990), a two-dimensional finite-element model based on a depth-averaged form of the Reynolds equations (Le Méhauté, 1976). The solution technique is discussed in King (1990). RMA2 is incorporated in the U.S. Army Corps of Engineers' TABS-2 modelling system (Thomas and McAnally, 1990). RMA2 and similar two-dimensional flow models such as FESWMS-2DH (Froehlich, 1988) have been used successfully in a variety of simulation applications (Bates *et al.*, 1992; Letter and Thibodeaux, 1991; Soong and Bhowmik, 1991; Deering, 1990; Gee *et al.*, 1990; MacArthur *et al.*, 1990; Froehlich, 1989; Wiche *et al.*, 1988). Model output includes flow depth and x and y components of depth-averaged velocity at each node in the network. The model can be used to simulate dynamic or steady-state conditions; for the present study, only steady-state conditions were simulated. Turbulent energy losses are represented in the model using the Boussinesq eddy-viscosity concept (Le Méhauté, 1976) in modelling the Reynolds stresses (King, 1990). The governing equations shown below are the continuity equation (1), the momentum equation in the x direction (2), and the momentum equation in the y direction (3):

$$\frac{\partial h}{\partial t} + \frac{\partial hu}{\partial x} + \frac{\partial hv}{\partial y} = 0 \quad (1)$$

$$\rho \left(h \frac{\partial u}{\partial t} + uh \frac{\partial u}{\partial x} + vh \frac{\partial u}{\partial y} \right) + h \frac{\partial}{\partial x} [\rho g(a + h)] - h\epsilon_{xx} \frac{\partial^2 u}{\partial x^2} - h\epsilon_{xy} \frac{\partial^2 u}{\partial y^2} + \rho S_{fx} + \tau_x = 0 \quad (2)$$

$$\rho \left(h \frac{\partial v}{\partial t} + uh \frac{\partial v}{\partial x} + vh \frac{\partial v}{\partial y} \right) + h \frac{\partial}{\partial y} [\rho g(a + h)] - h\epsilon_{yx} \frac{\partial^2 v}{\partial x^2} - h\epsilon_{yy} \frac{\partial^2 v}{\partial y^2} + \rho S_{fy} + \tau_y = 0 \quad (3)$$

where u and v are velocity components in the x and y directions; h is water depth; t is time; a is bed elevation; S_{fx} and S_{fy} are friction loss terms in the x and y directions; ρ is the density of water; g is the acceleration due to gravity; and ϵ_{xx} , ϵ_{xy} , ϵ_{yx} and ϵ_{yy} are eddy-viscosity coefficients. In the present study, eddy viscosity was assumed isotropic and all four coefficients were set at the same value. The τ_x and τ_y terms represent the combined influence of the Coriolis effect and wind shear, but these terms were assumed to be negligible for the purposes of this study.

Eddy viscosity can be parameterized in the model as a constant coefficient scaled by the sizes of the individual elements in the mesh; thus, the smaller elements have lower eddy viscosity. Large values of the eddy-viscosity coefficient have a pronounced damping effect on local velocity gradients. As smaller elements are used to represent areas of the flow field that are subjected to stronger gradients of velocity, depth and shear stress, the scaling reduces the damping effect of the eddy-viscosity coefficient on velocity gradients in these regions. In general, the value chosen for the constant coefficient is the smallest value that will allow a convergent solution. This is discussed in greater detail below.

The bottom shear stress term is based on a drag force formulation, e.g. shear stress is assumed to be the product of a drag coefficient and a squared-velocity term. This can be seen by taking the vector sum of the x and y components of shear stress described by Equations 4 and 5:

$$\rho S_{fx} = \rho \frac{gn^2}{h^{1/3}} u(u^2 + v^2)^{1/2} \quad (4)$$

$$\rho S_{fy} = \rho \frac{gn^2}{h^{1/3}} v(u^2 + v^2)^{1/2} \quad (5)$$

Bed roughness is parameterized using Manning's n or Chezy's C ; the option used in this study is the Manning coefficient, hence the form of the equations shown above.

FINITE-ELEMENT NETWORKS AND REPRESENTATION OF VALLEY TOPOGRAPHY

The finite-element networks used in the study were built using the program Viewnet (Shea, 1992). Input to this program was a series of valley cross-sections with control codes to guide the size and spacing of elements. In order to avoid computational difficulties it is important to avoid large elevation differences between nodes within an element, and therefore elements located along steep boundaries are much narrower than elements located in flatter parts of the flow field. In this study, elements along steep valley walls were constructed with maximum elevation differences of about 1.5 m.

Two alternative versions of the network were built; the configuration of elements in the vicinity of the fan location is illustrated in Figure 3. The version of the canyon reach without a fan (Reach 1) is straight and has a uniform cross-section with a top width of 160 m and a longitudinal gradient of 0.004. Total length of the reach used for flow simulation is 2550 m, extending from the upstream boundary at $x = 450$ m to the downstream boundary at $x = 3000$ m. A long entrance reach was included in both networks in order to ensure that the network would extend upstream of any potential backwater effects induced by the presence of the fan. The network used to simulate flow along Reach 1 has 4129 nodes and 1380 elements. Reach 2, the version of the network that includes a debris fan, is identical to Reach 1 in all respects other than the topographic features associated with the fan itself, which is attached to the left valley wall and extends from approximately 2300 to 2500 m on the longitudinal axis. No tributary valley is included in the simulation; I assume that the tributary junction would be an area of ineffective flow during any major flood along the main stem and therefore it is left out of the finite-element network for the sake of maintaining simple geometry. The network used here has 5876 nodes and 1977 elements. Orthographic projections of corresponding 500 m long sections from the two versions of the canyon reach illustrate the perturbation of valley topography caused by the fan (Figure 4).

RMA2 and other, similar two-dimensional finite-element flow models require specification of roughness coefficients for groups of elements, based on their physical characteristics. Therefore the question of whether or not to calculate a composite value of Manning's n for the entire cross-section does not arise here as it does when a one-dimensional step-backwater model is used. Values of Manning's n for the channel bed, channel-margin areas, and vegetated valley walls were specified as 0.03, 0.045 and 0.09. The upper surface of the fan was assigned the same roughness value as the valley walls.

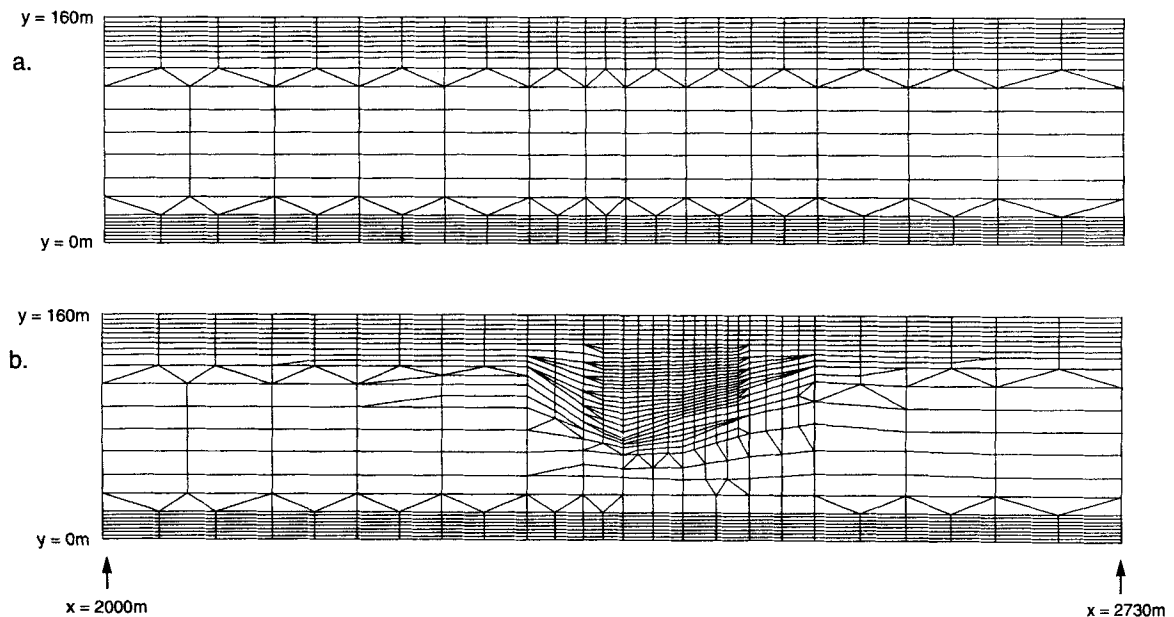


Figure 3. Partial views of finite-element networks used for simulation in this study: (a) Reach 1; (b) Reach 2

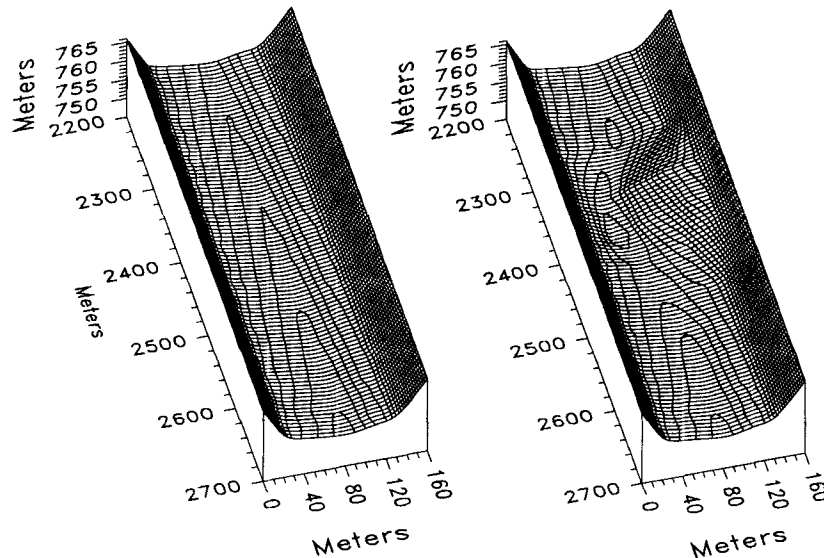


Figure 4. Perspective view of canyon topography used in flow simulation. All coordinates with respect to arbitrary datum. Contour interval 0.5 m. (a) Reach 1; (b) Reach 2

SIMULATION OF FLOOD FLOW

Several flow simulations were carried out for Reach 1, including discharges of 500, 750, 1000, 1500, 2000, 2500 and $3000 \text{ m}^3 \text{ s}^{-1}$. As flow along Reach 1 was subcritical at all discharges, the downstream boundary acted as a control section for locations further upstream. Because the reach is uniform in cross-section and longitudinal gradient, it was possible to adjust the stage at the downstream boundary until a uniform flow profile was attained along the entire length of the reach for each discharge value chosen. The resulting set of uniform flow profiles allows derivation of a stage–discharge relation for any location along the reach. The stage–discharge relation at the downstream boundary of Reach 1 was used to select stage values for each flow simulation along the downstream boundary of Reach 2. Flow simulations for discharges between 500 and $2000 \text{ m}^3 \text{ s}^{-1}$ were carried out for Reach 2; simulations of larger flows along this reach developed unstable perturbations and failed to converge properly.

In working with large flows routed through steep or irregular topography, great care must be taken in order to achieve a convergent solution. As noted by Bates *et al.* (1992), instabilities generally develop in limited areas of the flow field that have certain typical characteristics, including areas of steep lateral or longitudinal slope, sharp changes in the direction of flow, and areas where large volumes of water flow into small elements. In a simulation of a flow field with steeply sloping boundaries or with large areas of very shallow water, elements that are close to the projected elevation of the water surface in any part of the flow field may be subject to wetting and drying in successive iterations of the model as the shape of the water surface fluctuates in the search for a stable solution. A wetting/drying algorithm that turns entire elements off when the water surface drops below the elevation of any single boundary node can cause fairly abrupt changes in the predicted flow field from one iteration to the next. These changes may lead to computational instabilities that either prevent convergence or provide unrealistic solutions.

An alternative wetting/drying algorithm is available in recent versions of RMA2. The version containing this algorithm, known as the ‘marsh elements’ or ‘marsh porosity’ version, defines transition elements that may be thought of as partially wet when nodes on one side of the element are above the water surface while nodes on the other side are below the water surface. The algorithm allows smoother transitions toward convergent solution (Roig and King, 1990) and was utilized in the present study.

The types of instabilities mentioned by Bates *et al.* (1992) also can be mitigated somewhat by gradual adjustment of eddy-viscosity coefficients and of the water surface elevation at a downstream control section. It is generally necessary to start with a relatively flat longitudinal water-surface profile, which requires a beginning stage greater than normal depth along the downstream boundary. If this stage is gradually stepped down towards normal depth with each set of iterations, it becomes possible to achieve a convergent solution even in regions with high velocities and steep topography or complex boundaries.

Similarly, a relatively high value for the eddy-viscosity coefficient is used in the early iterations for any simulation, as this tends to damp out large lateral velocity gradients that might lead to unstable behaviour. The eddy-viscosity coefficient is also stepped down as the simulation approaches a convergent solution. As the concept of eddy viscosity is an artifact of the solution approach, there is no such thing as a 'true' value of the coefficient. Rodi (1984) points out that the eddy viscosity or effective diffusivity in a numerical model of a large water body generally accounts not only for the effects of turbulence, but also for numerical effects that are dependent on the scale of the grid, as well as dispersive transport due to non-uniformities of velocity. As was noted earlier, in practice the final value chosen for use in each simulation is the smallest value allowing a stable, convergent solution. However, there is some guidance in the literature regarding appropriate values, based largely on experimental measurement of heat or mass diffusion in open channels. Froehlich (1989) recommends a value on the order of $0.6 u_* h$, where $u_* h$ is shear velocity and h is water depth. Signell and Geyer (1991) note that eddy viscosities derived by Zimmerman (1986) for a coastal environment fall between 0.1 and $1.0 \text{ m}^2 \text{ s}^{-1}$ and are consistent with an empirical formula, $\epsilon = 0.2 u_* h$, suggested by Fischer *et al.* (1979); in their own study, Signell and Geyer adopt a constant eddy viscosity of $1.0 \text{ m}^2 \text{ s}^{-1}$.

Values used for the eddy-viscosity coefficient in this study yielded kinematic eddy viscosities ranging between about 0.02 and $0.18 \text{ m}^2 \text{ s}^{-1}$ when scaled by the long dimensions of individual elements in the mesh. Values of $0.2 u_* h$ calculated from model output generally ranged between 0.01 and $0.15 \text{ m}^2 \text{ s}^{-1}$, with a few nodes along the boundaries of the flow yielding values as low as 0.001 – $0.002 \text{ m}^2 \text{ s}^{-1}$. The larger values derived from model output generally corresponded to the larger values derived from the scaling formula, and a similar correspondence was observed for the smaller values. The assigned values for the eddy-viscosity coefficients therefore appear to be reasonable, at least to a first approximation.

RESULTS

Primary aspects of the flow simulation that are of concern here are: (1) hydraulics of flow around the fan as compared with the straight uniform reach; and (2) comparison of stage-discharge relations for the two reaches.

Shape of the water surface

Figure 5 allows a comparison of the shape of the water surface for simulations of the same discharge ($1000 \text{ m}^3 \text{ s}^{-1}$) in the two versions of the canyon reach. The water surface illustrated for Reach 1 has a nearly flat cross-section with a uniform gradient parallel to the longitudinal profile of the bed, whereas the water surface illustrated for Reach 2 is strongly perturbed as flow is diverted around the fan. The following features are observed.

- Water is ponded upstream of the fan.
- The water surface on the left side of the canyon (the right side from the reader's perspective) drops steeply as flow cascades around the front of the fan, reaching a minimum elevation a short distance downstream from the fan apex, then sloping upward again until it reaches a local maximum elevation near the 2500 m mark. From here, the water surface resumes a normal downstream gradient.
- Water flowing down the right side of the canyon (opposite the fan) has a smoother gradient; surface elevation begins to drop earlier than it does adjacent to the fan but never drops as steeply. Thus, the flow along the opposite wall appears to move down a ramp, whereas the flow adjacent to the fan appears to move into a chute.
- Continuing along the right side of the valley, the water surface reaches a local minimum elevation between locations 2550 and 2600 m, then slopes upward until it reaches a local maximum at about 2650 m.

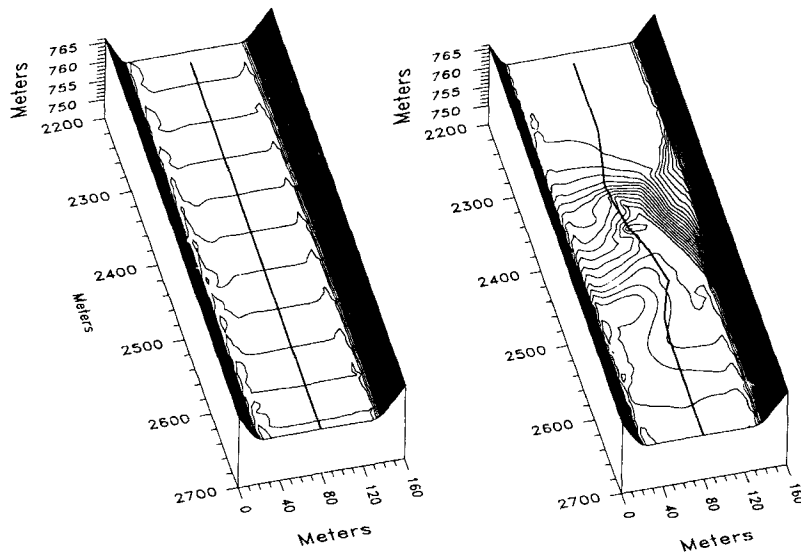


Figure 5. Simulated shape of water surface superimposed on valley topography for a flow of $1000 \text{ m}^3 \text{ s}^{-1}$. Contour interval 0.2 m . (a) Reach 1; (b) Reach 2. Distortions in water-surface contours adjacent to valley walls result from use of gridding algorithm to bridge transition from water surface to adjacent slope. Heavy lines oriented along longitudinal direction indicate locations of cross-sections used to compile data for Figures 10–12

The same basic pattern is observed over a range of discharge values but becomes more pronounced at higher discharges. If the fan profile were less steep, the higher discharges might overtop it completely and lead to a different flow pattern. The effects of overtopping are described by Kieffer (1985) and Schmidt (1990).

Flow field, velocity and shear-stress distribution

The observations listed above are reinforced by a perspective view of the flow vector field along Reach 2 (Figure 6). Two small areas of recirculating flow are shown in the regions of the flow field where an adverse gradient is observed. One recirculation cell is located along the downstream flank of the fan. The other is located further downstream along the right valley wall, where the flow initially diverted around the fan pulls back to the left and away from the right side of the canyon. Recirculation cells virtually disappeared in a simulation with eddy-viscosity coefficients 7.5 times greater than those used in the model run on which Figure 6 is based. Although local values of water-surface elevation and velocity were also sensitive to the choice of eddy-viscosity coefficients, the general shape of the water surface and of the velocity field remained the same across this range of coefficient values.

A comparison of the spatial distribution of resultant velocities (i.e. vector sum of u and v components) for a discharge of $1000 \text{ m}^3 \text{ s}^{-1}$ routed through the two alternative versions of the canyon reach is illustrated in Figure 7. As expected, the velocity pattern along Reach 1 is fairly simple. Maximum velocities over the deepest part of the channel are approximately 4.5 m s^{-1} . Along Reach 2, flow decelerates in the ponded area upstream of the fan and then quickly accelerates around the front of the fan. Peak velocities up to 6.9 m s^{-1} are predicted in the region of expanding flow a short distance downstream from the fan apex. Doubling of the eddy-viscosity coefficients causes virtually no change in the velocity field; increasing eddy viscosity by a factor of 7.5 causes some smoothing, with a maximum velocity of 6.4 m s^{-1} and slightly increased velocities along the margins of the flow. With increasing discharge, peak velocities are higher and extend slightly further downstream, but the basic pattern does not change.

Comparison of the spatial distribution of predicted shear stress (vector sum of Equations 4 and 5) at a discharge of $1000 \text{ m}^3 \text{ s}^{-1}$ highlights the difference between Reach 1 and Reach 2 even more strongly (Figure 8). The straight, uniform reach attains maximum bottom shear stresses of about 120 N m^{-2} , whereas

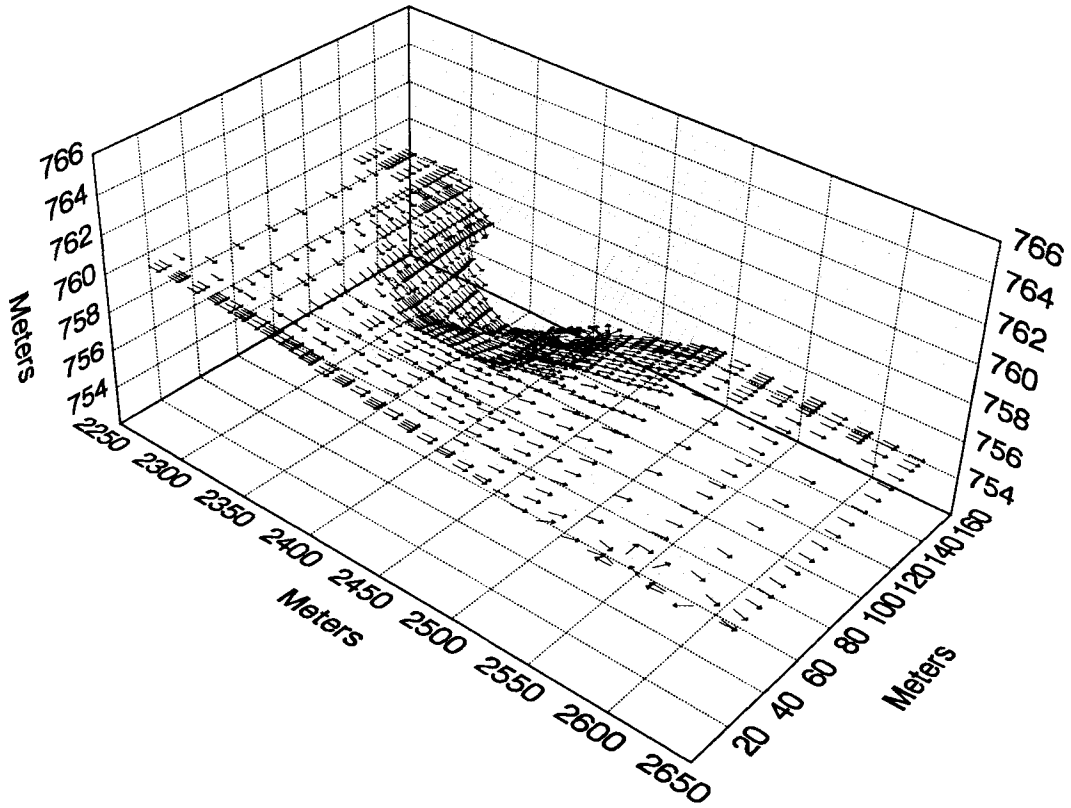


Figure 6. Vector field from simulation of $1000 \text{ m}^3 \text{ s}^{-1}$ flow in Reach 2. Vectors are not scaled to represent magnitude of resultant velocity

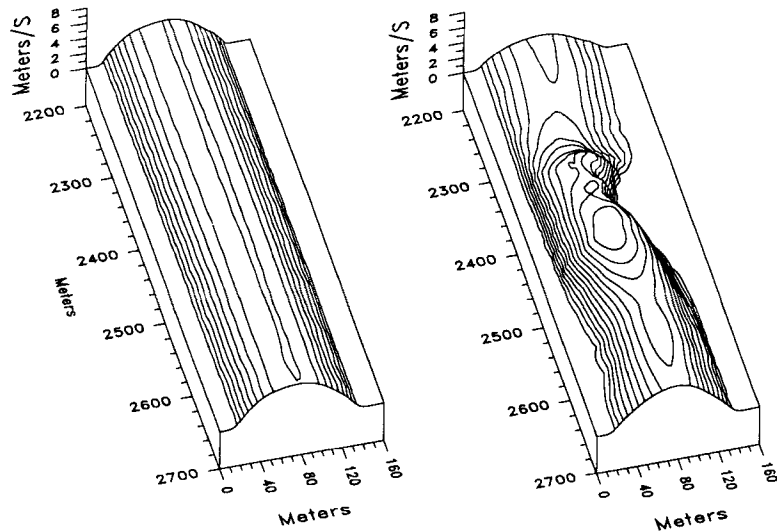


Figure 7. Perspective plots showing magnitude of resultant velocity for a flow of $1000 \text{ m}^3 \text{ s}^{-1}$. (a) Reach 1; (b) Reach 2. Contour interval 0.5 ms^{-1} ; minimum contour shown is 0.5 ms^{-1}

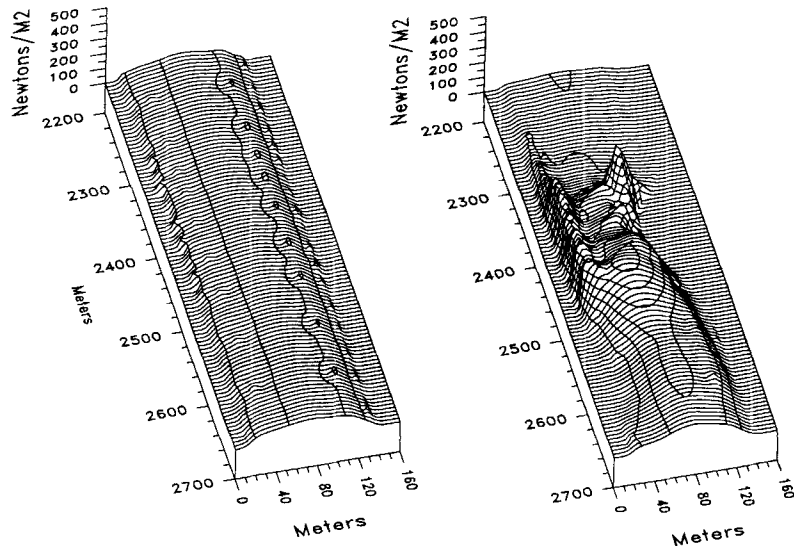


Figure 8. Perspective plots showing magnitude of resultant bed shear stress for a flow of $1000 \text{ m}^3 \text{ s}^{-1}$. (a) Reach 1; (b) Reach 2. Contour interval is 50 N m^{-2} ; minimum contour shown is 50 N m^{-2}

predicted maxima along canyon Reach 2 are more than three times greater. Predicted values are very low in the ponded area upstream of the fan but increase rapidly to a peak greater than 440 N m^{-2} at the point where flow along the fan margin descends down the 'chute' described earlier. (A 7.5-fold increase in eddy viscosity results in a maximum shear stress about 10 per cent lower at the same location.) The model assumption that vertical accelerations can be neglected may well be violated in this area of the flow field, and therefore the specific values predicted should be considered less reliable than the broad spatial patterns. Nevertheless, it is reasonable to expect elevated bed shear stress around the front of the fan as the flow enters the narrowest part of the constriction. A secondary peak exceeding 320 N m^{-2} is broader and is observed in the area of flow expansion past the apex of the fan where maximum velocities are indicated in Figure 7. A ridge of elevated shear stress values along the right valley wall opposite the fan is due to forcing of the high-velocity thread of flow around the fan, but the magnitude of the values shown is due, in part, to the high values of Manning's n specified for the valley walls. As shear stress is computed by taking the vector sum of Equations 4 and 5, it varies as the square of n .

The presence of supercritical flow in a portion of the flow field is indicated by a plot of the spatial distribution of Froude number $[u^2 + v^2/(gd)]^{1/2}$ (Figure 9). An area characterized by Froude numbers greater than 1 extends around the front of the fan and connects the two areas of maximum predicted shear stress identified in Figure 9. This is consistent with the cascading flow down the chute around the front of the fan, leading into the 'hole' in the water suggested by Figures 4 and 6. Presumably a hydraulic jump would be found somewhere along the portion of the channel characterized by an adverse water-surface gradient climbing out of the hole. The actual shape and location of such a jump cannot be reliably simulated under the assumptions that govern the model; although the results shown here represent a stable, convergent flow field, under most circumstances RMA2 produces spatial oscillations and unstable solutions when supercritical flow is modelled. Nevertheless, longitudinal profiles strongly suggest that a hydraulic jump would be present within this reach (Figure 10), especially at the higher discharges, and this is consistent with field observations of hydraulic jumps downstream of channel obstructions.

Stage-discharge relations

The perturbing effect of the fan on the shape of the water surface, discussed earlier in reference to Figures 5 and 6, is also illustrated using comparative longitudinal profiles for multiple discharge values (Figure 10).

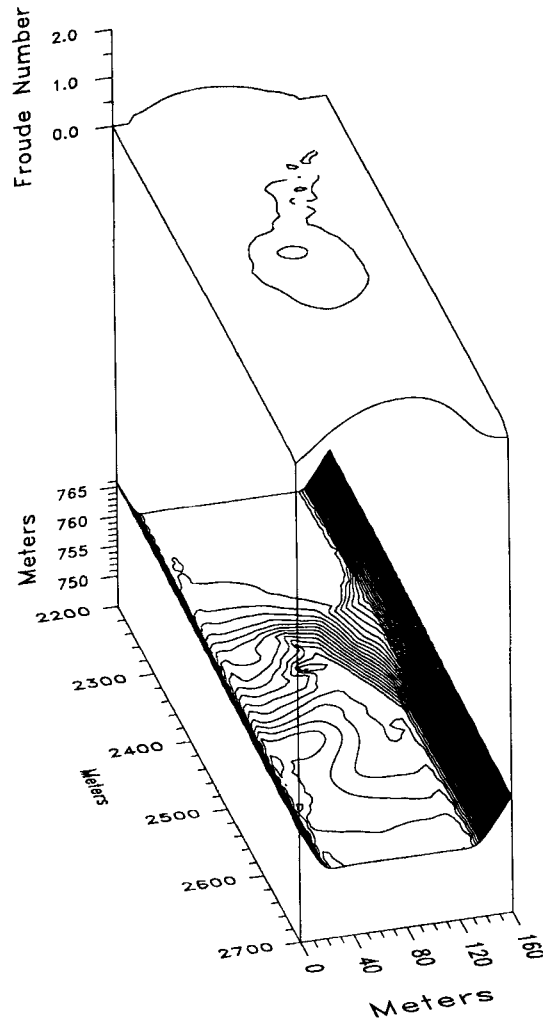


Figure 9. Perspective plots showing spatial distribution of Froude numbers greater than 1.0 along Reach 2 for a flow of $1000 \text{ m}^3 \text{ s}^{-1}$ (top), in relation to shape of water surface (bottom). Contour interval of upper plot is 0.5 and minimum contour shown is 1.0

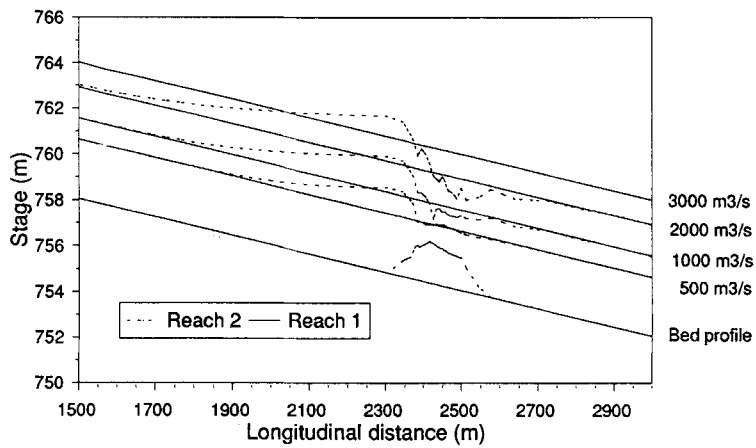


Figure 10. Comparative longitudinal profiles for selected discharge values; cross-section locations for Reach 1 and Reach 2 are shown in Figure 5

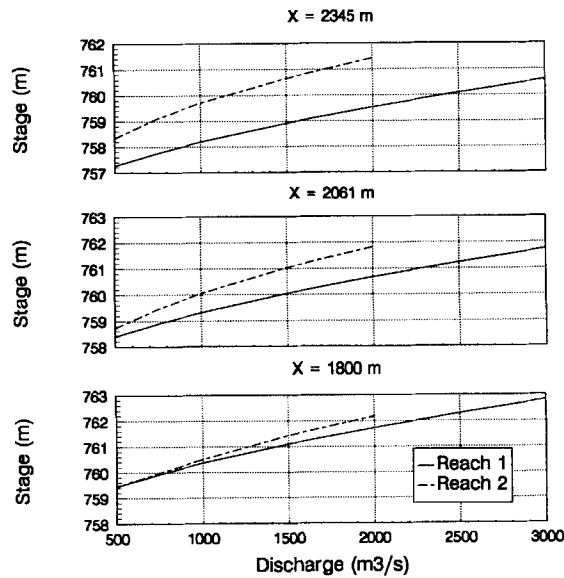


Figure 11. Comparison of stage–discharge relations at three longitudinal positions along the profiles shown in Figure 10

The ponding effect upstream of the fan and the longitudinal extent of the backwater curve can be seen by comparison of paired profiles for Reaches 1 and 2 at any of the discharge values shown. The magnitude of the backwater effect and its longitudinal extent increase with discharge, as one might expect. Perturbations in the water surface along the downstream slope of the fan are much more complex and unstable, as Figures 5 and 6 also show, but are damped out within a shorter distance.

Using the stage information shown in Figure 10, comparative stage–discharge relations or rating curves can be constructed for any location along the longitudinal profile. For any given stage one can readily compare the discharge values predicted when the fan is present, with those predicted when it is absent. The difference between curves is greatest just upstream from the fan, and the curves for the two alternative versions of the reach gradually converge for longitudinal positions further upstream (Figure 11). Note, for example, that at longitudinal position 2345 m, a stage of 760 m corresponds to a discharge of about $1150 \text{ m}^3 \text{ s}^{-1}$ along Reach 2; the same stage corresponds to a discharge of about $2400 \text{ m}^3 \text{ s}^{-1}$ along Reach 1. For most stages at this longitudinal position, the discharge value predicted by the stage–discharge relation along Reach 1 is about twice as large as the discharge value predicted along Reach 2. At longitudinal position 1800 m, however, a stage of 762 m corresponds to discharges of about $1875 \text{ m}^3 \text{ s}^{-1}$ along Reach 2 and $2250 \text{ m}^3 \text{ s}^{-1}$ (about 20 per cent higher) along Reach 1; the two curves are even closer at lower stages.

DISCUSSION

The spatial patterns of flow hydraulics described for Reach 2 in the preceding section are generally consistent with what is known about rapids associated with channel constrictions. A steep drop in the water surface occurs where flow is diverted around an obstruction; flow in this region accelerates downstream. A transition to supercritical flow may occur, accompanied by a local minimum in flow depth; this in turn is followed by a downstream transition back to subcritical flow, with velocity and shear stress maxima in the vicinity of the transition.

Where the constriction is created by a debris fan, truncation of the fan by lateral erosion may occur if flood discharges are large enough, as the velocities and shear stresses induced by the presence of the fan are locally up to several times greater than maximum values experienced in the absence of the fan. Thus a feedback effect is created by interaction of the flow field with the fan. This is consistent with Kieffer's (1985) observa-

tions of changes in Crystal Rapid and her additional observation that most rapids associated with major debris fans in the Grand Canyon appear to have width ratios adjusted to the hydraulics of large floods.

The occurrence of velocity and shear-stress peaks in and downstream from the narrowest part of the constriction is also consistent with observations indicating that scour holes tend to form at such locations. In the aftermath of the November 1985 flood in West Virginia, the deepest scour holes observed in the channel of the South Branch Potomac River and its major tributaries were formed at locations of truncated debris fans or other channel constrictions. For example, surveyed cross-sections at the site where the debris fan was removed in Figure 1d indicate channel depths of up to 3.6 m during summer low flow; maximum depths at most cross-sections along the same river rarely exceed 1 m for comparable low-flow conditions. The scour mark seen in plan view in Figure 2b formed on a floodplain in a region of local flow expansion immediately downstream from a debris fan. A gravel deposit on the floodplain just upstream is interrupted by the scour mark, presumably due to the steep increase in shear stress induced as flow was forced around the fan. The tendency toward formation of bars and gravel lobes immediately downstream from scour marks is also consistent with the patterns discussed above, as the rapid decrease of shear stress downstream from the stress peak would coincide with a decrease in local transport capacity.

Implications for palaeohydrologic reconstruction

The premise outlined in the introduction to this paper is that in some river canyons, local boundary conditions influencing flood profiles may change over time as debris fans are created and then modified or removed. The present example can serve as a hypothetical case to explore how changes in boundary conditions might affect the interpretation of palaeostage indicators to reconstruct past floods.

Let us assume, for the sake of argument, that Reach 2 represents boundary conditions at the time of some past flood, whereas Reach 1 represents boundary conditions at the present time, following removal of the debris fan. Let us assume further that a mark left by the flood is found and used to estimate the magnitude of the flood peak. How would the flood peak calculated using modern boundary conditions compare with the flood peak that actually left the mark? A longitudinal plot of this ratio (predicted Q to actual Q) can be constructed for any flood discharge within the range of flows that have been simulated (Figure 12). A mark located just upstream from the fan apex would generate the largest overestimates of the magnitude of the past flood, with predictions ranging from 190 to 230 per cent of the actual peak. With increasing distance upstream, the ratio decreases as we move out of the range of the backwater curve created by the fan.

Immediately downstream from the fan apex the ratio drops steeply and the details of the predicted water-surface profile in the vicinity of the 'hole' are probably less reliable. Furthermore, the extreme turbulence and the unsteady nature of the flow pattern that would occur at a similar site during a real flood would call into

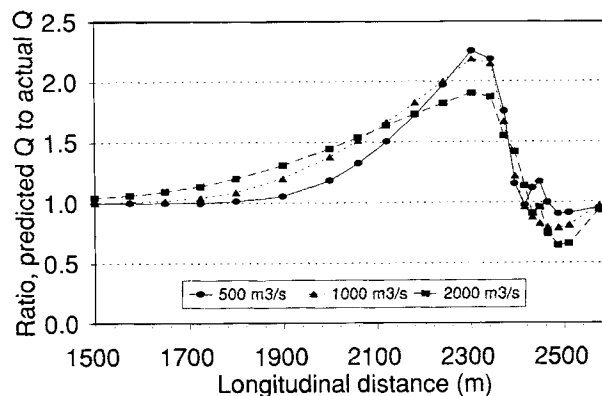


Figure 12. Ratio of discharge predicted for Reach 1 to discharge predicted for same stage at some longitudinal position along Reach 2. Definition of 'predicted' vs. 'actual' discharge is based on a scenario in which a flood mark created under boundary conditions prevalent along Reach 2 is applied to boundary conditions shown along Reach 1. See text for further discussion

question the interpretation of any marks found in this vicinity. At a distance sufficiently far downstream the effects of the perturbation created by the fan are probably negligible.

It is unlikely that an experienced investigator would try to reconstruct a past flood based on a single mark anywhere along the profile. Nor is it likely that a well-trained geomorphologist would fail to recognize evidence that large debris deposits had emanated from a tributary valley in the past, even if the debris fan itself were severely truncated or removed. However, if a fan were created and subsequently removed, there would inevitably be some uncertainty in reconstructing the boundary conditions that existed during the time that the fan was present. As tributary junctions and channel constrictions are among the most favourable sites for preservation of slack-water deposits (Kochel *et al.*, 1982; Partridge and Baker, 1987), the results suggest a need for careful consideration of all available field evidence. If the evidence indicates that debris deposits have been delivered to a tributary confluence in the past, then any use of hydraulic models for reconstruction of past floods should incorporate a sensitivity analysis considering alternative sets of boundary conditions.

There are additional complicating factors that may further confound efforts to reconstruct flood peaks. If a fan (or other obstruction) is substantially modified during the course of a flood, for example, then the stage–discharge relation needed for proper interpretation of residual flood marks may not reflect the starting or ending boundary conditions, but rather a transient, and therefore indeterminate, set of boundary conditions. If modifications of the boundary conditions begins on the rising stage of the hydrograph, it is also possible that the highest flood marks left behind are not representative of the discharge peak; the stage

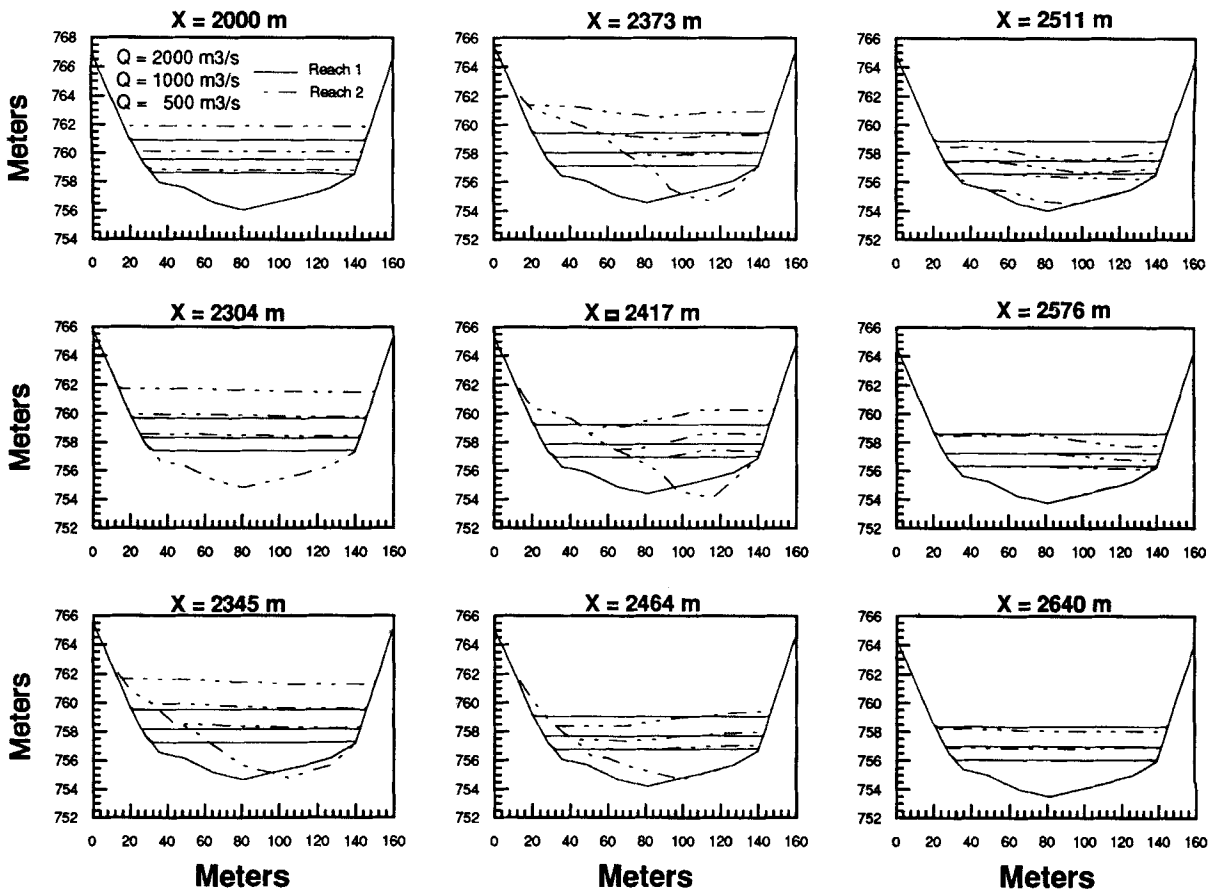


Figure 13. Comparative cross-stream profiles for the two reaches at three different discharge levels for a series of cross-sections at indicated locations

may have begun falling upstream from a constriction as the shape of the constriction changed, even though discharge was still increasing. Local debris jams or transient obstructions may temporarily block some or all of the valley cross-section, leading to local superelevation of the water surface followed by a drop in water level if the obstruction is breached or removed. All of these phenomena have the potential to produce high-water marks that are not indicators of peak discharge.

Cross-stream gradients and implications for use of one-dimensional flow models

The analysis of stage–discharge relations in Figures 10–12 is based on a single longitudinal section along the canyon. Therefore, any reconstruction of flood discharge based on these relations is subject to an additional important source of error. Strong cross-stream gradients in the water surface are clearly present when flood flows are routed through Reach 2 (Figures 5 and 6); consequently, the stage–discharge relations predicted for particular points along a longitudinal profile may not be valid all the way across the channel. Furthermore, the strength and direction of the cross-stream gradients may change in a short longitudinal distance, particularly downstream from the fan. This is illustrated in a series of cross-sections representing longitudinal positions along the canyon between locations $x = 2000$ m and $x = 2640$ m (Figure 13).

Several hundred metres upstream from the fan ($x = 2000$ m), comparison of the shape of the water surface for three different flows routed through Reaches 1 and 2 indicates that there is a substantial backwater effect due to the fan but no significant cross-stream gradient. Just upstream from the fan ($x = 2304$ m), the backwater effect is greater and there is a small dip to the right, which increases downstream ($x = 2345$ m) and causes a cross-stream elevation difference of about 0.5 m. Approaching the fan apex ($x = 2373$ m), the dip shifts from the right back towards the channel centre near the beginning of the chute, and just 44 m further downstream ($x = 2417$ m) it shifts over the left margin with a total elevation difference exceeding 1 m at a discharge of $1000 \text{ m}^3 \text{ s}^{-1}$. Between $x = 2417$ m and $x = 2576$ m, the cross-stream gradient first stabilizes, then shifts back to the right channel margin, slowly flattening again approaching the 2640 m mark. Although some of the cross-stream undulations could be artifacts of the model, the major features persist over a range of discharges and eddy-viscosity coefficients, and the velocity vectors do not exhibit the types of spatial fluctuations that are characteristic of unstable solutions. In any case, there are almost certainly even more complex and possibly larger-amplitude undulations in the form of standing waves and other, transient disturbances that would be observed in the channel if real flows of the magnitude discussed here were to occur.

In the presence of a fan or other comparable constriction, or even in the presence of a tight bend in the valley, the possibility of such marked cross-stream gradients presents a formidable obstacle for reconstruction of the hydraulic conditions present during a large flood. Williams and Costa (1988) suggest that when superelevation is apparent from comparison of flood marks on the outside and inside of a channel bend, a formula from Chow (1959) can be used to estimate mean velocity and therefore to reconstruct discharge. However, they also produce the following caveat: ‘Due to possible wave action, irregularities in cross-sectional geometry, and many other factors, the error with this method easily could be 50%’ (Williams and Costa, 1988, p. 68). Other authors interested in estimating past flood peaks have used methods that are based on the one-dimensional energy equation. Chief among these are the step-backwater models, the best-known of which is the Army Corps of Engineers’ HEC-2 Water Surface Profiles program (Hydrologic Engineering Center, 1982). These models assume a flat water surface within any cross-section oriented perpendicular to the main flow direction. O’Connor and Webb (1988) note that ‘for exceedingly complex channel geometries, the assumption of one-dimensional gradually varied flow may not be valid . . .’ (p. 395). The difficulty lies in deciding, in each individual case, what channel geometry is simple enough that a one-dimensional simulation can be relied upon. Of the two alternative test reaches simulated in this paper, Reach 1 is simple enough that a one-dimensional model should provide a satisfactory solution. Reach 2 is characterized by a single large perturbation, and its geometry is otherwise quite simple; yet the two-dimensional shape of the water surface shown in Figures 5, 6 and 13 cannot be simulated by a one-dimensional model, and some characteristics of the flow may not be accurately simulated even by a two-dimension model.

It is worth noting that whereas every whitewater enthusiast can describe typical patterns of flow and the general shape of the water surface as a river flows through a rapid, available measurements of the shape of

the water surface are generally not detailed enough to provide a good data set for verification. Flume studies conducted with laser-doppler velocimeters allow the collection of more comprehensive data sets, but the flows and boundary conditions being studied are not generally comparable to those that exist during large floods. All we generally have to work with are individual high-water marks or palaeostage indicators left behind along the margins of the flow, and not all of these marks are indicators of peak stage or of peak discharge. There are often spatial gaps where the water-surface profile must be estimated by interpolation. It is therefore not surprising that the models applied to simulate the available field data are themselves based on relatively simple assumptions. More detailed field data documenting flood flow patterns are needed.

The growing availability of two-dimensional flow models and of high-speed desktop computers capable of running them opens up an avenue for more careful exploration of complex perturbations in the water surface that may occur along rivers where one-dimensional models have been utilized in the past. As the data and the amount of labour required to assemble a mesh for two-dimensional finite-element simulation are considerably greater than for step-backwater simulation, it would not be desirable or practical to replace the one-dimensional approach entirely. Nor is the two-dimensional model used in this study a panacea. A more sophisticated turbulence closure is warranted in many situations (ASCE Task Committee on Turbulence Models in Hydraulic Computation, 1988), though the models that have been most widely used and most readily available are limited to the approach described earlier. In addition, it must be recognized that many flows are fully three-dimensional; the secondary currents that are critically important components of flow through a meander bend are not simulated in a two-dimensional depth-averaged model. The velocity fields simulated by models such as the one used here are not as reliable as the water-surface profiles and should be treated as incremental improvements over the one-dimensional simulations rather than as accurate reflections of reality. Even where secondary currents are not important, there are places where the assumptions of two-dimensional flow are strongly enough violated that only a three-dimensional simulation can adequately represent the physics of flow. However, to the extent that a two-dimensional simulation can help to resolve what is happening along parts of a flood profile that cannot otherwise be successfully modelled, an approach utilizing both one- and two-dimensional models may be feasible. Further research comparing the results of both types of simulations with detailed verification data sets is warranted.

ACKNOWLEDGEMENTS

This paper benefited from helpful comments by Robert D. Jarrett, Robert B. Jacobson and an anonymous reviewer, and from discussions about interpretation of model output with Charlie Berger, Barbara Donnell and David Richards of the U.S. Army Corps of Engineers Waterways Experiment Station. Interpretations and conclusions are, of course, the sole responsibility of the author. Research for this paper was partially funded by National Science Foundation Grant SES-8722442. Computer time was provided by the Pittsburgh Supercomputing Center under Grant EAR91005P.

REFERENCES

- ASCE Task Committee on Turbulence Models in Hydraulic Computation. 1988. 'Turbulence modeling of surface water flow and transport: Part I', *Journal of Hydraulic Engineering*, **114**, 970–991.
- Baker, V. R., Kochel, R. C., Patton, P. C. and Pickup, G. 1983. 'Palaeohydrologic analysis of Holocene flood slackwater sediments', in Collinson, J. D. and Lewin, J. (Eds), *Modern and Ancient Fluvial Systems*, Special Publication of the International Association of Sedimentologists 6, Blackwell Scientific Publications, Oxford, 229–239.
- Bates, P. D., Anderson, M. G., Baird, L., Walling, D. E. and Simm, D. 1992 'Modelling floodplain flows using a two-dimensional finite element model', *Earth Surface Processes and Landforms*, **17**, 575–588.
- Chow, V. 1959. *Open-Channel Hydraulics*, McGraw-Hill, New York, 680 pp.
- Deering, M. K., 1990, 'Practical applications of 2-d hydrodynamic modeling', in Chang, H. H. and Hill, J. C. (Eds), *Hydraulic Engineering: Proceedings of the 1990 National Conference*, American Society of Civil Engineers, New York, 755–760.
- Fischer, H. B., List, E. J., Koh, R. C. Y., Imberger, J. and Brooks, N. J. 1979. *Mixing in Inland and Coastal Waters*, Academic Press, San Diego.
- Froehlich, D. C. 1988. *Finite element surface water modeling system: 2-dimensional flow in the horizontal plane—User's Manual*, Federal Highway Administration Publication No. FHWA-RD-88-177.
- Froehlich, D. C., 1989. 'Hydraulic analysis of the Schoharie Creek bridge', in Ports, M. A. (Ed), *Hydraulic Engineering: Proceedings of the 1989 National Conference*, American Society of Civil Engineers, New York, 887–992.

- Gee, D. M., Anderson, M. G. and Baird, L. 1990. 'Large-scale floodplain modelling', *Earth Surface Processes and Landforms*, **15**, 513–523.
- Graf, W. L. 1979. 'Rapids in canyon rivers', *Journal of Geology*, **87**, 533–551.
- Hydrologic Engineering Center. 1982. *HEC-2 Water Surface Profiles: User's Manual*, U.S. Army Corps of Engineers, Davis, California.
- Kieffer, S. W. 1985. 'The 1983 hydraulic jump in Crystal Rapid: implications for river-running and geomorphic evolution in the Grand Canyon', *Journal of Geology*, **93**, 385–406.
- King, I. P. 1990. *Program Documentation: RMA2—a Two Dimensional Finite Element Model for Flow in Estuaries and Streams, Version 4.3*, Resource Management Associates, Lafayette, California.
- Kochel, R. C. 1987. 'Holocene debris flows in central Virginia', in Costa, J. E. and Wieczorek, G. F. (Eds), *Debris Flows/Avalanches: Process, Recognition, and Mitigation*, Geological Society of America, Reviews in Engineering Geology, VII, 139–155.
- Kochel, R. C. and Baker, V. R. 1982. 'Paleoflood hydrology', *Science*, **215**, 353–361.
- Kochel, R. C., Baker, V. R. and Patton, P. C. 1982. 'Paleohydrology of southwestern Texas', *Water Resources Research*, **18**, 1165–1183.
- Le Méhauté, B. 1976. *An Introduction to Hydrodynamics and Water Waves*, Springer-Verlag, New York.
- Leopold, L. B. 1969. *The rapids and the pools—Grand Canyon*, U.S. Geological Survey Professional Paper 669, 131–145.
- Letter, J. V. Jr and Thibodeaux, B. J. 1991. 'Modelling of wetland hydrodynamics and transport in coastal Louisiana', in Shane, R. M. (Ed.), *Hydraulic Engineering: Proceedings of the 1991 National Conference*, American Society of Civil Engineers, New York, 274–279.
- MacArthur, R. C., Dexter, J. R., Smith, D. J. and King, I. P. 1990. 'Two-dimensional finite element simulation of the flooding characteristics in Kawaiui Marsh, Hawaii', in Chang, H. H. and Hill, J. C. (Eds), *Hydraulic Engineering: Proceedings of the 1990 National Conference*, American Society of Civil Engineers, New York, 664–669.
- Miller, A. J. 1990. 'Fluvial response to debris associated with mass wasting during extreme floods', *Geology*, **18**, 599–602.
- O'Connor, J. E. and Webb, R. H. 1988. 'Hydraulic modeling for paleoflood analysis', in Baker, V. R., Kochel, R. C. and Patton, P. C. (Eds), *Flood Geomorphology*, John Wiley and Sons, New York, 393–402.
- O'Connor, J. E., Webb, R. H. and Baker, V. R. 1986. 'Paleohydrology of pool-and-riffle pattern development: Boulder Creek, Utah', *Geological Society of America Bulletin*, **97**, 410–420.
- Partridge, J. and Baker, V. R. 1987. 'Paleoflood hydrology of the Salt River, Arizona', *Earth Surface Processes and Landforms*, **12**, 109–125.
- Rodi, W. 1984. *Turbulence Models and Their Application in Hydraulics—a State of the Art Review*, International Association for Hydraulic Research.
- Roig, L. C. and King, I. P. 1990. *A finite-element model to simulate flows in tidal flats*, Department of Civil Engineering, University of California, Davis (Unpublished paper).
- Schmidt, J. C. 1990. 'Recirculating flow and sedimentation in the Colorado River in Grand Canyon, Arizona', *Journal of Geology*, **98**, 709–724.
- Shea, C. 1992. *Viewnet: an Interactive Utility for Viewing Finite Element Networks*, version 1.0, Department of Geography and Environmental Engineering, Johns Hopkins University, Baltimore.
- Signell, R. P. and Geyer, W. R. 1991. 'Transient eddy formation around headlands', *Journal of Geophysical Research*, **96**(C2), 2561–2575.
- Soong, T. W. and Bhowmik, N. G. 1991. 'Two-dimensional hydrodynamic modeling of a reach of the Mississippi River in Pool 19', in Shane, R. M. (Ed.), *Hydraulic Engineering: Proceedings of the 1991 National Conference*, American Society of Civil Engineers, New York, 900–905.
- Thomas, W. A. and McAnally, W. H. Jr. 1990. *User's Manual for the Generalized Computer Program System: Open-Channel Flow and Sedimentation, TABS-2*, U.S. Army Engineer Waterways Experiment Station, Vicksburg, Mississippi.
- Wiche, G. J., Gilbert, J. J., Froehlich, D. C. and Lee, J. K. 1988. *Analysis of alternative modifications for reducing backwater at the Interstate Highway 10 crossing of the Pearl River near Slidell, Louisiana*, U.S. Geological Survey Water-Supply Paper 2267.
- Williams, G. P. and Costa, J. E. 1988. 'Geomorphic measurements after a flood', in Baker, V. R., Kochel, R. C. and Patton, P. C. (Eds), *Flood Geomorphology*, John Wiley and Sons, New York, 65–77.
- Zimmerman, J. T. F. 1986. 'The tidal whirlpool: a review of horizontal dispersion by tidal and residual currents', *Netherlands Journal of Sea Research*, **20**, 133–154.